Gain and G/T of Multielement Receive Antennas with Active Beamforming Networks

Ulrich R. Kraft, *Senior Member, IEEE*

***Abstract*—A basic system-level model for the gain and G/T of active multielement receive antennas is presented that covers arbitrary beamforming networks and direct radiating arrays, as well as array-fed systems with one or more focusing elements (reflectors or lenses). Since the model is based on measurable parameters and uses definitions, which are consistent with conventional communication system analysis terms, it can be applied directly to the analysis and design of systems using such antennas and can be used to support the specification, design, and test of such antennas as well. Measurement possibilities for the basic parameters are briefly discussed and the characteristic parameters of generic active beamforming networks are derived and compared. Finally, the impact of the different parameters on the overall antenna gain and G/T is illustrated by one application example that covers a reconfigurable multifeed reflector antenna with selectable beamwidth. The presented theory has been verified successfully in the frame of a classified EHF antenna development whose details cannot be reported here.**

***Index Terms*—Active antennas, beamforming networks, direct radiating arrays, multifeed reflector antennas, phased arrays.**

I. Introduction

ACTIVE receive antennas with beamforming capabilities become increasingly attractive for a variety of applications such as military SATCOM, mobile communications, etc., since their technology basis constantly improves whereas the performance and flexibility requirements of modern systems still increase. Such antennas can be direct-radiating arrays or array-fed systems with one or more focusing elements (reflectors or lenses) and comprise active beamforming networks that perform low-noise signal amplification, amplitude-and phase weighting of the individual radiator signals and the combination of these signals at the common antenna output port.

Apart from the technical challenges associated with the implementation of active beamforming antennas, one basic problem in this field is the antenna characterization on system level, which should permit a simple treatment of these antennas by conventional system analysis and design tools and should provide useful, measurable parameters for their specification, design, and test. Whereas pattern parameters such as beamwidth, polarization, sidelobe level, etc., do not require basically new considerations, gain and G/T are more complex since they depend on the radiation focusing properties, the amplitude- and phase weighting, as well as the internal amplifications and losses of the active antenna. The situation for the simple case of a passive receive antenna with or without a focusing optics is shown in Fig. 1, which presents a signal/noise model of the antenna/receiver combination for use within system analysis tools. The antenna is connected to the receiver at the antenna/receiver interface (ARI), where the conventionally defined antenna gain is available. The incoming signal is amplified with respect to an ideal (loss- and sourceless) isotropic radiator by the directivity D depending on the antenna pattern, and is then attenuated by the internal loss L_A, which describes the net effect of all losses within the antenna. Noise contributions arise from the total noise received by the antenna, the internal antenna noise generated by the losses, and the noise of the receiver, which are described by the conventional antenna temperature T_A [1], the effective internal noise temperature given by $(L_A - 1)T_0$ for the worst case of purely ohmic losses, and the effective receiver input temperature $T_{\rm rec}$, respectively. Accordingly, the total antenna gain at the ARI and the G/T of the antenna/receiver combination are given by

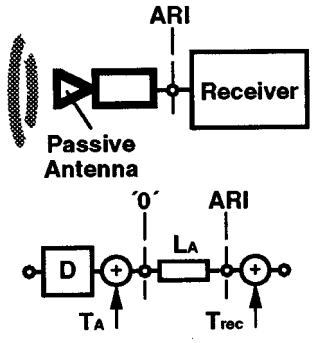

Fig. 1. Basic system level model for a conventional, passive receive antenna.

$$G = D/L_A \tag{1}$$

and

$$\begin{aligned} G/T &= D/(T_A + (L_A - 1)T_0 + L_A T_{\rm rec}) \\ &= G/(T_A/L_A + (1 - 1/L_A)T_0 + T_{\rm rec}) \end{aligned} \tag{2}$$

wherein T_0 denotes the physical temperature of the antenna. For $T_A = T_0$ or $L_A = 1$ (no losses), (2) reduces to the well-known and simple formula

$$G/T = G/(T_A + T_{\rm rec}). \tag{3}$$

In case of active antennas having several reception chains, i.e., several sources of signal amplification, signal attenuation, and noise, the situation is much more complex leading to the fact that even the basic definition for the gain of an active receive antenna is not yet finally established [2]–[4]. Previously

Manuscript received August 24, 1998; revised January 7, 2000.

The author is with Astrium GmbH, D-81663 Munich, Germany (e-mail: ulrich.kraft@astrium-space.com).

Publisher Item Identifier S 0018-926X(00)10836-1.

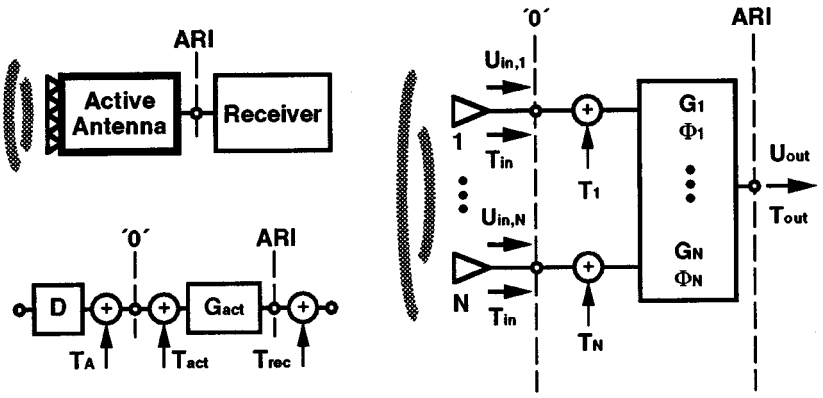

Fig. 2. Basic system level model for an arbitrary active multielement receive antenna (one channel system version and N-channel antenna version).

published considerations on the gain and G/T of such antennas are limited to different phased array configurations, where the directivity change due to amplitude weightings (taper) can be directly expressed as a function of the applied weights [4], [5]. Earlier, the author has reported some limited results on a more general approach covering both phased arrays and reflector-type antennas [6] but a general treatment of the subject is not yet available from the open literature.

The goal of this paper is to provide a general formulation for the gain and G/T of multielement receive antennas with active beamforming networks (BFNs), which covers different configurations of the BFN such as active weighting via active amplitude control elements and passive weighting via nonuniform combiners (cf. [5]), direct-radiating arrays, as well as array-fed systems with one or more focusing elements. Here, the antenna gain is understood as the amplification of the signal power level at the output port of the active antenna compared to the signal power level at the output port of an ideal, i.e., loss- and sourceless, isotropic radiator receiving the same incoming wave. According to this definition, the gain of an active antenna has the same meaning as the gain of a passive type, which permits its direct integration into conventional system analysis methods and its direct measurement using conventional procedures. The developed formulation for G/T covers the entire reception chain, i.e., it includes the amplification and noise impact of the active antenna, as well as the noise contribution from the following receiver.

The general models are described in Section II of this paper, where measurement possibilities for the characteristic parameters are also briefly discussed. The parameters of generic BFNs are then derived and compared in Section III. Finally, Section IV shows one application example for a multifeed reflector antenna, which illustrates the impact of the different antenna parameters on the overall gain and G/T performance. The validity of the developed models has been verified successfully in the frame of a classified EHF antenna development whose details cannot be reported here.

II. Basic System-Level Model

A general system-level model for arbitrary direct radiating or focused multielement receive antennas with active beamforming networks is shown in Fig. 2, which presents both a one-channel version of the antenna/receiver combination for use in system analysis tools, as well as a multichannel version of the antenna itself for the corresponding antenna analysis. As aforementioned, the antenna is connected to the receiver at the ARI, where the total antenna gain is available.

Taking the one-channel model, the incoming signals are amplified with respect to an ideal isotropic radiator by the directivity D of the generated overall antenna pattern and the internal active gain $G_{\rm act}$ describing the total effect of all losses and amplifications. Noise contributions arise from the total noise received by the antenna, the internal antenna noise generated by losses and active elements, and the noise of the receiver, which are described by T_A, the effective internal noise temperature $T_{\rm act}$, and $T_{\rm rec}$, respectively. Here it should be noted that T_A depends on the overall (signal) antenna pattern as long as the active aperture is small compared to the correlation length of the received, filtered noise. Otherwise, decorrelation effects have to be taken into account, which lead to deviations between the effective antenna pattern for signal and noise reception. Such aspects are covered in more detail in the Appendix. The total antenna gain at the ARI and the G/T of the antenna/receiver combination are given by

$$G = DG_{\rm act} \tag{4}$$

and

$$\begin{aligned} G/T &= D/(T_A + T_{\rm act} + T_{\rm rec}/G_{\rm act}) \\ &= G/(G_{\rm act}(T_A + T_{\rm act}) + T_{\rm rec}) \end{aligned} \tag{5}$$

which implies that for a reasonable active gain $G_{\rm act}$, the overall antenna gain is larger than the directivity, as expected from an active antenna, and that the receiver has only a limited impact on the overall G/T since its noise contribution is reduced by $G_{\rm act}$. Since the gain and G/T definitions applied in the model are consistent with the usual conventions of communication systems analysis, the model can be directly integrated into existing system analysis tools. Moreover, its characteristic parameters G, D, $G_{\rm act}$, and $T_{\rm act}$ can be derived from measurements that enable their use for the specification, analysis, design, and test of active multielement receive antennas. Whereas G can be measured directly by conventional gain measurement methods, D can be

obtained by integrating measured antenna pattern, which finally permits the determination of $G_{\rm act}$ by using (4). In addition, G/T can be measured directly by applying the conventional on/off-method to a compact antenna test range, which then enables the determination of $T_{\rm act}$ from (5), if T_A is known, $T_{\rm rec}$ has been measured using conventional techniques, and $G_{\rm act}$ has been determined as described before.

The dependence of the characteristic parameters $G_{\rm act}$ and $T_{\rm act}$ on internal gains, losses, and noise contributions can be determined from the multichannel antenna model also shown in Fig. 2. The antenna comprises N radiator elements with or without a focusing optics delivering the signal voltages $U_{{\rm in},1}$ to $U_{{\rm in},N}$ and the equally assumed noise temperatures $T_{\rm in}$. These elements are connected to a N-channel "internal" antenna described by overall channel gains G_1 to G_N, overall channel phases Φ_1 to Φ_N and effective channel input noise temperatures T_1 to T_N leading to an output signal voltage $U_{\rm out}$ and an output noise temperature $T_{\rm out}$ given by

$$U_{\rm out} = \sum_{n=1}^{N} U_{{\rm in},n} \exp(j\Phi_n)\sqrt{G_n} \tag{6}$$

and

$$T_{\rm out} = \sum_{n=1}^{N} (T_{\rm in} + T_n) G_n. \tag{7}$$

In order to derive the expressions for $G_{\rm act}$, this antenna configuration is compared to an equivalent, ideal (loss- and sourceless, $G_{\rm act} = 1$) antenna generating the same radiation pattern, which acts as a theoretical reference case. For this reference case, the corresponding output voltage $U_{\rm out'}$ can be written as

$$U_{\rm out'} = \sum_{n=1}^{N} U_{{\rm in},n} \exp(j\Phi_n)\sqrt{1/L_{n'}} \tag{8}$$

wherein $(1/L_{n'})$ denote normalized channel transmissions that differ from the channel gains G_n only by a multiplicative constant $G_{\rm norm}$, but that must satisfy

$$\sum_{n=1}^{N} (1/L_{n'}) = 1 \tag{9}$$

because of the absence of losses and sources within the ideal antenna. Based on this theoretical reference, which corresponds, e.g., to a passive, lossless antenna using a nonuniform coupler-type network with $(1/L_{n'})$ being the coupling coefficients of the different channels, $U_{\rm out}$ and G_n can be written as denormalized versions of $U_{\rm out'}$ and $(1/L_{n'})$ according to $U_{\rm out} = U_{\rm out'}\sqrt{G_{\rm act}}$ and $G_n = G_{\rm norm}(1/L_{n'})$. This permits a determination of the internal active gain $G_{\rm act}$ from (6), (8), and (9) to

$$G_{\rm act} = G_{\rm norm} = \sum_{n=1}^{N} G_n \tag{10}$$

which also provides a second possibility for the experimental determination of $G_{\rm act}$, if the channel gains G_n can be measured. The effective internal noise temperature $T_{\rm act}$ can be derived from the one-channel system model and the N-channel antenna model, if a noise temperature $T_{\rm in}$ is assumed at the interface "0" of both models and the corresponding output noise temperatures at the ARI are compared

$$T_{\rm out} = (T_{\rm in} + T_{\rm act})G_{\rm act} = \sum_{n=1}^{N} (T_{\rm in} + T_n) G_n. \tag{11}$$

Using (10) and (11), $T_{\rm act}$ is given by

$$T_{\rm act} = \sum_{n=1}^{N} T_n G_n \Big/ \sum_{n=1}^{N} G_n = \sum_{n=1}^{N} T_n G_n \Big/ G_{\rm act}. \tag{12}$$

Whereas the general models and equations presented so far describe an arbitrary active multielement receive antenna by overall parameters for the "internal" antenna ($G_{\rm act}$, $T_{\rm act}$) which cover all elements of an individual channel in an integral way without restrictions on the channel configuration, most practically relevant antenna types consist of two main assemblies: a passive radiator system (with or without a focusing optics) and an active beamforming network (BFN). From a practical point-of-view, this situation makes a second, dedicated description desirable that identifies the individual impacts of these two main assemblies on antenna gain and G/T, permits the derivation of characteristic parameters especially for the BFN and provides measurement possibilities for these parameters. If the passive radiator system exhibits a total loss per channel and a corresponding total transmission phase per channel, which can be assumed as equal for all channels, and if both the radiator system and the beamforming network are sufficiently matched, such a dedicated description can be derived from the one-channel system model and the N-channel antenna model described before, whereas larger differences between channels or significant mismatch make the use of the general models (Fig. 2) more appropriate.

The corresponding dedicated models are shown in Fig. 3, where the radiator system is characterized by a total loss L_A per channel covering also a possible focusing optics, whereas the corresponding transmission phases have been set to zero. At the new interface "1," the radiator system is connected to the BFN, which is described by its channel gains, phases, and input noise temperatures $G_{n'}$, $\phi_{n'}$, and $T_{n'}$ and its overall effective gain and noise temperature $G_{\rm BFN}$ and $T_{\rm BFN}$. In order to derive the modified equations for gain and G/T, $G_{\rm act}$, and $T_{\rm act}$ are expressed as a function of $G_{\rm BFN}$, $T_{\rm BFN}$, and L_A based on a comparison of Figs. 2 and 3, which leads to

$$G_{\rm act} = G_{\rm BFN}/L_A \tag{13}$$

and

$$T_{\rm act} = (L_A - 1)T_0 + L_A T_{\rm BFN}. \tag{14}$$

Herein, T_0 denotes the physical temperature of the radiator system and L_A has been assumed again as a purely ohmic loss. Finally, the overall gain and G/T of the antenna can be written as

$$G = (D/L_A)G_{\rm BFN} \tag{15}$$

and

$$G/T = D/(T_A + (L_A - 1)T_0 + L_A T_{\rm BFN} + L_A T_{\rm rec}/G_{\rm BFN}) \tag{16}$$

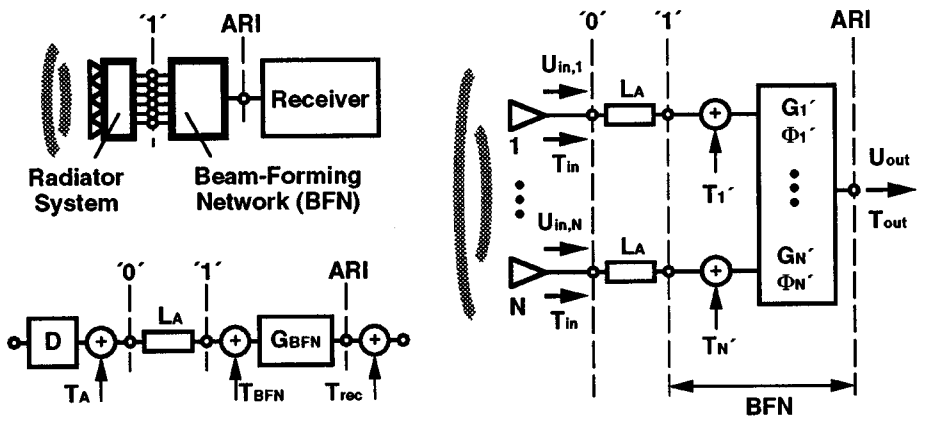

Fig. 3. Basic system level model for an arbitrary multielement receive antenna comprising a separable passive radiator system and an active beamforming network (one channel system version and N-channel antenna version).

using (4), (5), (13), and (14). Equations (15) and (16) reduce to the simple formulas of the passive case given by (1) and (2), if an ideal, loss and sourceless BFN (i.e., $G_{\mathrm{BFN}} = 1, T_{\mathrm{BFN}} = 0$) is considered and permit an indirect determination of G_{BFN} and T_{BFN} from the measured parameters G, G/T, and D, if L_A and T_A are known with sufficient accuracy. Vice versa, L_A can be determined from (15) and (16), if G_{BFN} and T_{BFN} are obtained by the independent measurements described below and T_A is known.

The dependence of the effective BFN gain G_{BFN} on the corresponding BFN channel characteristics can be derived by a comparison of Figs. 2 and 3 leading to $G_{n'} = G_n L_A$ and by use of (13) leading finally to

$$G_{\mathrm{BFN}} = G_{\mathrm{act}} L_A = \sum_{n=1}^{N} G_n L_A = \sum_{n=1}^{N} G_{n'}. \qquad (17)$$

This provides a simple possibility for an independent measurement of G_{BFN} by measuring the BFN input-to-output transmission coefficients $G_{n'}$ via a network analyzer and calculating G_{BFN} according to (17). Finally, T_{BFN} can be determined by assuming a homogeneous input noise temperature $T_{\mathrm{in}'}$ at the interface "1" of both the one-channel and the N-channel model and comparing the two output noise temperatures at the ARI

$$T_{\mathrm{out}} = (T_{\mathrm{in}'} + T_{\mathrm{BFN}}) G_{\mathrm{BFN}} = \sum_{n=1}^{N} (T_{\mathrm{in}'} + T_{n'}) G_{n'} \qquad (18)$$

which leads to

$$T_{\mathrm{BFN}} = \sum_{n=1}^{N} T_{n'} G_{n'} \Big/ \sum_{n=1}^{N} G_{n'} = \sum_{n=1}^{N} T_{n'} G_{n'} \Big/ G_{\mathrm{BFN}}. \qquad (19)$$

A not very obvious measurement possibility for T_{BFN} arises, if the BFN is fed at one input port k with an input noise T_{IN} ($T_{\mathrm{in}'} = T_{\mathrm{IN}}$ for $n = k$), whereas all other input ports are terminated ($T_{\mathrm{in}'} = T_0$ for $n <> k$) generating a two-port network with an effective noise temperature T_{BFN^*} and an input-to-output gain $G_{k'}$. In this case, (18) delivers

$$T_{\mathrm{out}} = (T_{\mathrm{IN}} + T_{\mathrm{BFN}^*}) G_{k'} = (T_{\mathrm{IN}} - T_0) G_{k'} + \sum_{n=1}^{N} (T_0 + T_{n'}) G_{n'} \qquad (20a)$$

or

$$T_{\mathrm{out}} = (T_{\mathrm{IN}} - T_0) G_{k'} + G_{\mathrm{BFN}} (T_0 + T_{\mathrm{BFN}}) \qquad (20b)$$

wherein T_0, T_{BFN}, and G_{BFN} denote the physical temperature and the characteristic parameters of the BFN. If T_{BFN^*} is directly measured by usual two-port methods and $G_{k'}$ and G_{BFN} are derived from network-analyzer tests, T_{BFN} can be obtained by

$$T_{\mathrm{BFN}} = (G_{k'}/G_{\mathrm{BFN}})(T_0 + T_{\mathrm{BFN}^*}) - T_0. \qquad (21)$$

III. Characteristic Parameters of Generic Beamforming Networks

In the previous section, the impact of the effective BFN gain (G_{BFN}) and the effective BFN noise temperature (T_{BFN}) on the gain and G/T of multielement receive antennas has been derived whereby arbitrary BFNs characterized only by their channel gains and phases $G_{n'}$, $\Phi_{n'}$ and their equivalent noise temperatures $T_{n'}$ have been considered. In order to close the gap between these general formulations and particular BFN configurations used in practice, now the dependence of G_{BFN} and T_{BFN} on the BFN architecture and the corresponding assembly performances is investigated where two steps are taken. Since practical BFNs consists, in general, of a number of electronic chains followed by a uniform or nonuniform power combiner but the implementation of amplitude and phase distributions can be performed by one of these main elements or shared between them, at first, a generic architecture is considered and corresponding generic expressions for G_{BFN} and T_{BFN} are derived. Based on these generic expressions, the two most popular configurations called "active weighting" and "passive weighting" network are then investigated in detail with the goal to derive detailed expressions for G_{BFN} and T_{BFN}

as functions of the electronic chain and combiner parameters for these cases. Hereby, it is assumed that the radiator system loss L_A and the corresponding transmission phases are either sufficiently uniform to permit a separate BFN consideration according to Fig. 3 or are treated as part of the BFN, which would imply $G_{\text{act}} = G_{\text{BFN}}$ and $T_{\text{act}} = T_{\text{BFN}}$. Additionally, both the radiator system and the BFN are assumed to be matched.

The generic architecture as shown in Fig. 4 consists of N identical electronic chains followed by a $N:1$-combiner. These chains typically comprise low-noise amplifiers (LNA), variable-gain-amplifiers (VGA), and variable phase-shifters (VPS), which are used to perform a signal preamplification, a flexible and reconfigurable setting of the aperture amplitude- and phase distribution, and/or a compensation of possible channel imperfections. They are described by a common nominal gain G_0, actual gains $G_{e,1}$ to $G_{e,N}$ given by a reduction of the nominal gain by L_1 to L_N, transmission phases $\Phi_{e,1'}$ to $\Phi_{e,N'}$, and actual input noise temperatures $T_{e,1}$ to $T_{e,N}$ given by a nominal temperature T_e plus an amplitude-setting dependent increase $\delta T_e(L_n)$. The following combiner can be a uniform or nonuniform type depending on the architecture and performs the summation of the individual channel outputs plus a possible fixed or limited switchable amplitude- and phase weighting. It is characterized by overall combiner losses $L_{C,1}$ to $L_{C,N}$ covering divider losses as well as ohmic and other loss factors, transmission phases $\Phi_{c,1'}$ to $\Phi_{c,N'}$ and input noise temperatures T_{C1} to T_{CN} representing the internally generated noise from ohmic losses and possible active elements. For this overall configuration, the total transmission gain and phase of one BFN channel ("1" to ARI) and the corresponding effective input noise temperature are given by

$$\begin{aligned} G_{n'} &= G_{e,n}/L_{C,n} = G_0(1/L_n)(1/L_{C,n}) \\ &= G_0(1/L_{\text{tot},n}) \qquad (22a) \\ \Phi_{n'} &= \Phi_{e,n'} + \Phi_{C,n'} \qquad (22b) \\ T_{n'} &= T_{e,n} + T_{C,n}/G_{e,n} \\ &= T_e + \delta T_e(L_n) + T_{C,n}L_n/G_0 \qquad (22c) \end{aligned}$$

leading to an effective BFN gain and noise temperature [(17), (19)] of

$$G_{\text{BFN}} = G_0 \sum_{n=1}^{N}(1/L_n)(1/L_{C,n}) = G_0 \sum_{n=1}^{N}(1/L_{\text{tot},n}) \qquad (23)$$

$$\begin{aligned} T_{\text{BFN}} = {} & T_e + \sum_{n=1}^{N}(\delta T_e(L_n)/L_{\text{tot},n}) \Big/ \sum_{n=1}^{N}(1/L_{\text{tot},n}) \\ & + (1/G_0)\sum_{n=1}^{N}(T_{C,n}/L_{C,n}) \Big/ \sum_{n=1}^{N}(1/L_{\text{tot},n}). \qquad (24) \end{aligned}$$

As shown by (22a) and (22b) the final aperture amplitude and phase distribution depends on the net effect of the electronic chains and combiner. Here, an active weighting via the chains permits a flexible antenna reconfiguration whereas a passive weighting via a tailored combiner can be less complex but delivers only a fixed or limited switchable distribution. For most practical cases, where the amplitude distribution is set by the chains *or* the combiner, (23) and (24) can be simplified significantly, which is shown below for the two most popular BFN configurations.

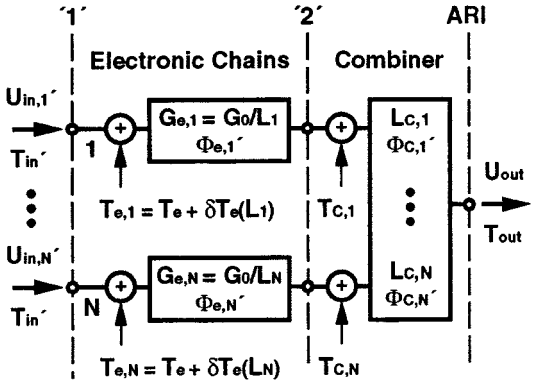

Fig. 4. System level model for a generic active beamforming network.

One very popular BFN architecture is the "*active weighting*" BFN where a fully flexible amplitude/phase control is performed via the electronic chains, whereas the signal combination is done by a uniform $N:1$-power combiner ($L_{C,1} = L_{C,2} = \cdots = L_{C,N}$, $\Phi_{c,1'} = \Phi_{c,2'} = \cdots = \Phi_{c,N'} = 0°$). For this configuration, (23) can be simplified to

$$G_{\text{BFN}} = G_0(N/L_C)(G_W/N) \qquad (25a)$$

with

$$(G_W/N) = (1/N)\sum_{n=1}^{N}(1/L_n) \qquad 0 \le (G_W/N) \le 1 \qquad (25b)$$

and

$$\begin{aligned} (1/L_C) &= (1/L_{C,1}) = (1/L_{C,2}) = \cdots = (1/L_{C,N}) \\ &= (1/N)\sum_{n=1}^{N}(1/L_{C,n}) \qquad (25c) \end{aligned}$$

wherein the normalized weighting gain G_W/N characterizes the total impact of an actively formed amplitude taper on the BFN gain without a dependence on the actual configuration, the number of antenna elements etc. The parameter reaches its maximum $(G_W/N = 1)$ for an uniform amplitude distribution and decreases for stronger tapers which implies a corresponding maximum BFN gain for the uniform case. The parameter $(1/L_C)$ describes the effective combiner loss which is equal to the individual channel losses $L_{C,n}$ in case of an uniform combiner. Similarly, the effective BFN temperature (24) can be simplified to

$$T_{\text{BFN}} = T_e + (N/G_W)(DT_e + T_C/G_0) \qquad (26a)$$

with

$$\begin{aligned} DT_e &= (1/N)\sum_{n=1}^{N}\delta T_e(L_n)/L_n \qquad (26b) \\ T_C &= (1/N)\sum_{n=1}^{N} T_{C,n} \\ &= \sum_{n=1}^{N}(T_{C,n}/L_{C,n}) \Big/ \sum_{n=1}^{N}(1/L_{C,n}). \qquad (26c) \end{aligned}$$

Herein DT_e and T_C describe the impact of the chain noise increase $\delta T_e(L_n)$ and the combiner noise sources $T_{C,n}$, respectively, whereby the effective combiner noise temperature T_C is the equivalent to T_{BFN}, if an isolated combiner is considered as a "BFN," and becomes equal to the individual sources $(T_C = T_{C,n})$, if all noise sources $T_{C,1}$ to $T_{C,N}$ are equal.

For most practical cases, $\delta T_e(L_n)$ can be approximated by a linear function according to

$$\delta T_e(L_n) = (L_n - 1)\Delta T_e \tag{27a}$$

leading to

$$DT_e = (1 - G_W/N)\Delta T_e \tag{27b}$$

and finally to

$$T_{\mathrm{BFN}} = (T_e + T_C/G_0) + (N/G_W - 1)(\Delta T_e + T_C/G_0). \tag{28}$$

In this case, the impact of an actively generated amplitude taper is again described by G_W/N, leading to the minimum BFN noise temperature for the uniform amplitude distribution $(G_W/N = 1)$.

In many practical cases, the uniform combiner is realized as a cascade of passive $2:1$ combiner stages, which implies a divider loss N' per channel, an additional path loss L_p per channel accounting for the net-effect of internal add-on losses, and an overall combiner loss L_C given by

$$L_C = N' L_p. \tag{29}$$

Herein, N' is equal to the number of elements N, if N complies to $N = 2^n$, and is equal to the next larger number which complies, otherwise. A combiner with $N <> 2^n$ physical input ports is, therefore, equivalent to a $N':1$ combiner with $(N'-N)$ terminated input ports. The corresponding input noise temperatures $T_{C,1}$ to $T_{C,N}$ are generated by the ohmic path losses L_p of N' combiner channels plus the additional noise of $(N'-N)$ terminated input ports and can be assumed as equal. They can be determined by a comparison of the output noise temperature T_{out} generated by the real $N':1$ combiner with equal input noise temperatures T_{IN} at the N open ports and the physical temperature T_0 at the $(N'-N)$ terminated ports with the corresponding figure $T_{\mathrm{out}'}$ of an equivalent $N:1$ combiner with equal input noise temperatures T_{IN} and equal noise sources T_C for all N channels

$$\begin{aligned} T_{\mathrm{out}} &= (NT_{\mathrm{IN}} + N'(L_p - 1)T_0 + (N' - N)T_0)/L_C \\ &= T_{\mathrm{out}'} = (NT_{\mathrm{IN}} + NT_C)/L_C \end{aligned} \tag{30a}$$

leading to

$$T_C = ((N'/N)L_p - 1)T_0. \tag{30b}$$

The second popular BFN architecture is the "*passive weighting*" BFN where a fixed or limited switchable amplitude distribution is generated via a tailored nonuniform combiner. In this case, the electronic chains comprise low-noise amplifiers to obtain a signal preamplification and can also contain variable phase shifters to set a desired, flexible aperture phase distribution, e.g., to realize low-sidelobe phased arrays. The chains are described by a constant nominal gain G_0, transmission phases $\Phi_{e,1'}$ to $\Phi_{e,N'}$, and actual input noise temperatures $T_{e,1}$ to $T_{e,N}$, which are equal to the nominal temperature T_e since all chains operate without the gain reductions of the active weighting architecture. The desired aperture amplitude distribution is realized by the nonuniform $N:1$-combiner which usually comprises different cascaded couplers and is characterized by overall combiner losses $L_{C,1}$ to $L_{C,N}$ and input noise temperatures $T_{C,1}$ to $T_{C,N}$. If a flexible phase-steering is not required, the channel phases $\Phi_{1'}$ to $\Phi_{N'}$ are fix and can be generated also by the nonuniform combiner itself ($\Phi_{c,n'} <> 0°$), which is a standard approach for passive multifeed reflector antennas. In both cases, (23) can be simplified to

$$G_{\mathrm{BFN}} = G_0(N/L_C) \tag{31a}$$

with

$$(1/L_C) = (1/N)\sum_{n=1}^{N}(1/L_{C,n}) \tag{31b}$$

wherein $(1/L_C)$ describes again the effective combiner loss. Similarly, the effective BFN temperature (24) can be simplified to

$$T_{\mathrm{BFN}} = T_e + (T_C/G_0) \tag{32a}$$

with

$$T_C = \sum_{n=1}^{N}(T_{C,n}/L_{C,n}) \Bigg/ \sum_{n=1}^{N}(1/L_{C,n}) \tag{32b}$$

wherein T_C denotes again the effective combiner noise temperature, which becomes equal to the individual noise sources $(T_C = T_{C,n})$, if these sources are equal.

In many practical cases, the combiner is realized as a cascade of passive coupler stages, which implies that the overall combiner losses $L_{C,1}$ to $L_{C,N}$ are given by the product of normalized divider losses $L_{1'}$ to $L_{N'}$ satisfying (9) and additional ohmic path losses L_p per channel. Here, (31b) leads to

$$(1/L_C) = (1/N)\sum_{n=1}^{N}(1/L_p L_{n'}) = (1/NL_p) \tag{33}$$

because of (9), i.e., no energy is lost by the weighting itself except those parts absorbed by the ohmic losses. Assuming the ohmic path losses L_p as the only source of internally generated noise, i.e., equal noise sources $T_{C,n}$ for all channels, these sources and T_C are given by

$$T_{C,n} = T_C = (L_p - 1)T_0. \tag{34}$$

A comparison of the "active weighting" and "passive weighting" architecture in terms of G_{BFN}, T_{BFN}, and the most important assembly parameters is provided in Table I, which covers a general amplitude distribution and the uniform case. Apart from the limited amplitude flexibility of the passive weighting architecture, differences exist for both the gain and the noise temperature behavior of the configurations which affect the overall antenna gain and the G/T. As shown in Table I, a passive weighting BFN behaves like an active weighting configuration that is operated for a uniform amplitude distribution $(G_W/N = 1)$, i.e., the passive weighting BFN always obtains

TABLE I
COMPARISON OF KEY PARAMETERS FOR ACTIVE AND PASSIVE WEIGHTING BFNs

BFN Type		active weighting	passive weighting
BFN Gain G_{BFN}	general case	$G_0 (N/L_C) (G_W/N)$	$G_0 (N/L_C)$
	uniform	$G_0 (N/L_C)$	$G_0 (N/L_C)$
BFN Noise Temperature T_{BFN}	general case	$(T_e + T_C/G_0) + (N/G_W - 1)(\Delta T_e + T_C/G_0)$	$(T_e + T_C/G_0)$
	uniform	$(T_e + T_C/G_0)$	$(T_e + T_C/G_0)$
Parameters General Case	(G_W/N)	$(1/N)\sum_{n=1}^{N}(1/L_n)$	—
	$(1/L_C)$	$(1/N)\sum_{n=1}^{N}(1/L_{Cn}) = (1/L_{Cn})$	$(1/N)\sum_{n=1}^{N}(1/L_{Cn})$
	T_C	$\sum_{n=1}^{N}(T_{Cn}/L_{Cn}) / \sum_{n=1}^{N}(1/L_{Cn}) = (1/N)\sum_{n=1}^{N} T_{Cn}$	$\sum_{n=1}^{N}(T_{Cn}/L_{Cn}) / \sum_{n=1}^{N}(1/L_C$
Parameters Special Case	Combiner Type	cascade of passive 2 : 1 combiner stages	cascade of passive coupler stages
	L_{Cn}	$N' L_p \xrightarrow{N = 2^n} N L_p$	$L_n' L_p$
	L_C	$N' L_p \xrightarrow{N = 2^n} N L_p$	$N L_p$
	T_C	$((N'/N)L_p - 1)T_0 \xrightarrow{N = 2^n} (L_p - 1)T_0$	$(L_p - 1)T_0$

maximum BFN gain and minimum noise temperature, whereas the performance of active weighting versions degrades with increasing amplitude taper. Since the BFN gain also reduces the overall noise impact of the receiver following the antenna [(16)], the receiver impact on G/T is usually larger for the active weighting configuration, as already pointed out in [5] for phased arrays. Moreover, the BFN gain contributes to the overall antenna gain [(15)] leading to lower antenna gains for an active amplitude control (cf. [4], [5]), which can be compensated by a corresponding increase of the nominal chain gain G_0. Accordingly, the sensitivity of T_{BFN} to the applied amplitude setting can be minimzed by using larger LNA gains within the electronic chains leading to smaller setting dependences of the chain-noise temperatures (ΔT_e), and by using a larger nominal chain gain (G_0) to reduce the impact of the combiner noise (T_C). For the important case of passive combiners, the table shows that the combiner parameters L_C and T_C are similar for active- and passive-weighting configurations and become equal, if the number of inputs N complies to $N = 2^n$, and the ohmic path losses L_p are equal for both architectures.

IV. APPLICATION EXAMPLE: RECONFIGURABLE Ka-BAND SPOTBEAM ANTENNA WITH ZOOMING CAPABILITY

In order to provide an application example that illustrates the impact of the different antenna parameters on the overall gain and G/T performance, a reconfigurable active Ka-band reflector antenna is considered which permits a change of the realized beamwidth by means of a suitable beamforming network. Such an antenna is of interest for satellite applications, where an adaption of the illuminated coverage area size (zooming) can be desired to enhance the system flexibility [7], [8]. If a fully flexible beamsize is required, an active-weighting BFN is neccessary, which is assumed for the basic configuration in the following considerations. For reasons of comparison, however, a switchable passive weighting BFN as implemented, e.g., for the

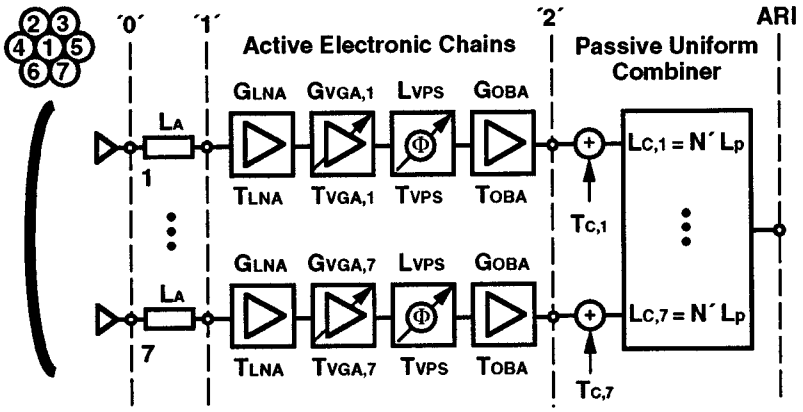

Fig. 5. Configuration of a configurable Ka-Band spotbeam antenna.

Hemi-Zone antennas of the INTELSAT VIII satellite series [9], [10] is also investigated, since it can be an alternative, if only a small number of beam sizes is desired.

The basic configuration of the antenna, presented in Fig. 5, comprises an offset parabolic reflector with a diameter of 81.4 λ (81.4 cm for 30 GHz) and a F/D of 0.76, which is illuminated by seven feedhorns arranged in a hexagonal cluster. Through the associated BFN, the centerhorn (#1) is always operated with the nominal gain G_0 of the corresponding electronic chain ($L_1 = 1$), whereas all six ringhorns (#2 to #7) are used with the reduced gain G_0/L_R (L_2 to $L_7 = L_R$) leading to a normalized weighting gain $G_{W/N}$ [cf. (25b)] of

$$G_W/N = (1/N)(1+(N-1)/L_R) = (1/7)(1+6/L_R). \quad (34)$$

By changing the ring-taper L_R, the corresponding antenna pattern can be adjusted to a desired beamwidth or coverage size, which is illustrated for two cases by the pattern cuts shown in Fig. 6(a). If the ringtaper is increased from 2.7 dB to 17.3 dB, the half-power beamwidth (HPWB) of the antenna decreases from 2.3° to 0.9° [Fig. 6(b)], which causes an increase of the corresponding directivity at the 3 dB points of the pattern (edge-of-coverage or EOC directivity) from 34.8 dBi to 41.3 dBi [Fig. 6(c)]. This behavior is typical for a single-reflector (or lens) multifeed antenna, where an increasing amplitude taper over the multifeed aperture leads to a beamwidth decrease (directivity increase) in contrast to the case of direct radiating or magnified (double reflector/lens) arrays, where an increasing taper causes a beamwidth increase (directivity decrease).

The associated active-weighting BFN shown in Fig. 5 comprises seven active electronic chains that are the cascade of a low-noise amplifier (LNA), a variable-gain amplifier (VGA) implementing the desired amplitude weighting, a variable-phase shifter (VPS) for phase-error corrections of the corresponding BFN channel, and a possible output-buffer amplifier (OBA) for the enhancement of the overall chain amplification. These components are described by their gains or losses G_{LNA}, G_{VGA}, L_{VPS}, and G_{OBA} and their effective input noise temperatures T_{LNA}, T_{VGA}, T_{VPS}, and T_{OBA}, which are equal in all chains for the LNAs, VPSs, and OBAs, whereas the VGAs are set to different amplifications in order to implement the desired amplitude weighting. These settings lead to the VGA parameters

$$G_{\mathrm{VGA},\,n} = G_{\mathrm{VGA}}/L_n \quad (35a)$$

and

$$T_{\mathrm{VGA},\,n} = T_{\mathrm{VGA}} + (L_n - 1)\Delta T_{\mathrm{VGA}} \quad (35b)$$

which result in the following effective parameters of the electronic chains

$$G_0 = G_{\mathrm{LNA}} G_{\mathrm{VGA}} G_{\mathrm{OBA}} / L_{\mathrm{VPS}} \quad (36a)$$

$$T_e = T_{\mathrm{LNA}} + (T_{\mathrm{VGA}}/G_{\mathrm{LNA}}) + (T_{\mathrm{VPS}}/G_{\mathrm{LNA}}G_{\mathrm{VGA}}) + (L_{\mathrm{VPS}}T_{\mathrm{OBA}}/G_{\mathrm{LNA}}G_{\mathrm{VGA}}) \quad (36b)$$

and

$$\Delta T_e = (\Delta T_{\mathrm{VGA}}/G_{\mathrm{LNA}}) + (T_{\mathrm{VPS}}/G_{\mathrm{LNA}}G_{\mathrm{VGA}}) + (L_{\mathrm{VPS}}T_{\mathrm{OBA}}/G_{\mathrm{LNA}}G_{\mathrm{VGA}}). \quad (36c)$$

Here, an approximation of $\delta T_e(L_n)$ by $(L_n - 1)\Delta T_e$ according to (27a) is possible, since the VGA noise temperatures can be approximated accordingly, which has been checked in practice during a classified EHF antenna development. Assuming dual-stage HEMT amplifiers for the LNAs, OBAs, and the input stages of the VGA assembly, a combined analog/digital approach for the VPSs and an overall realization of the BFN in integrated technology, G_{LNA}, G_{VGA}, G_{OBA}, and L_{VPS} can be assumed to 16 dB, 18 dB, 18 dB, and 16 dB at 30 GHz, whereas the corresponding noise temperatures and noise figures are given by 365 K, 472 K, 446 K, and 11 450 K and 3.5 dB, 4.1 dB, 4.0 dB, and 16 dB, respectively. Using $\Delta T_{\mathrm{VGA}} = 1.3$ K, these figures result in overall chain parameters $G_0 = 36$ dB, $T_e = 388.5$ K, and $\Delta T_e = 11.7$ K for the configuration shown in Fig. 5 and $G_0 = 18$ dB, $T_e = 381.4$ K, and $\Delta T_e = 4.6$ K for an alternative configuration, where the OBAs have been removed. The uniform power combiner of the BFN is assumed as a passive 8 : 1 combiner realized in MIC technology having one terminated input port, which uses a cascade of 2 : 1 Wilkinson power combiners with an ohmic loss of 1.5 dB per stage at 30 GHz. This leads to ohmic path losses L_p of 4.5 dB per channel, an overall combiner loss L_C of 13.5 dB [(29)] and an effective combiner noise temperature T_C of 655.2 K [(30b)] assuming a physical temperature of 295 K.

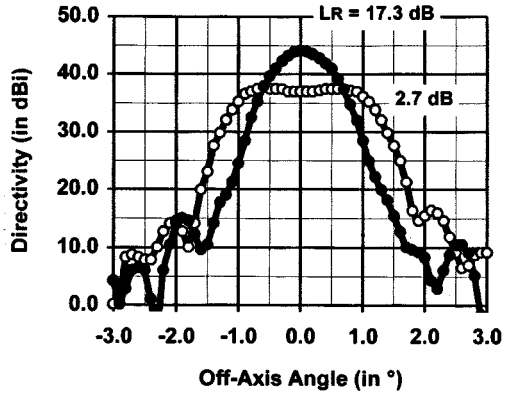

(a)

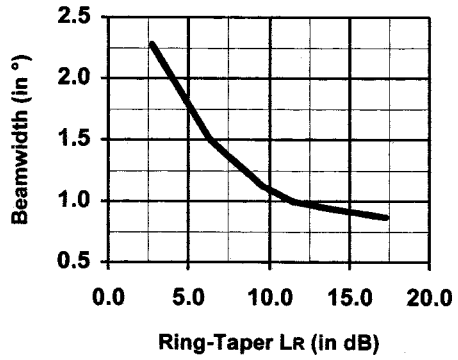

(b)

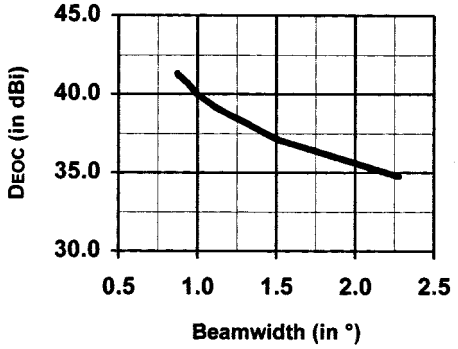

(c)

Fig. 6. Radiation properties of the reconfigurable spotbeam antenna depending on the applied amplitude taper. (a) Radiation pattern cuts. (b) Half-power beamwidth (HPBW). (c) Antenna directivity at the 3 dB points of the pattern (EOC-directivity).

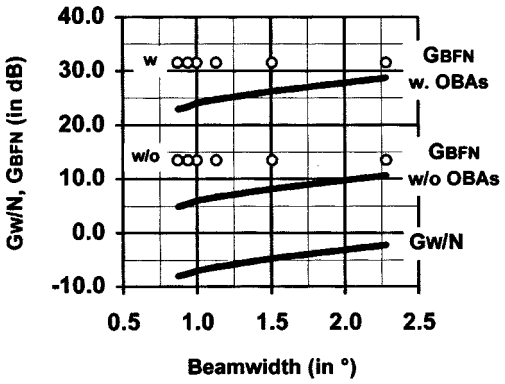

(a)

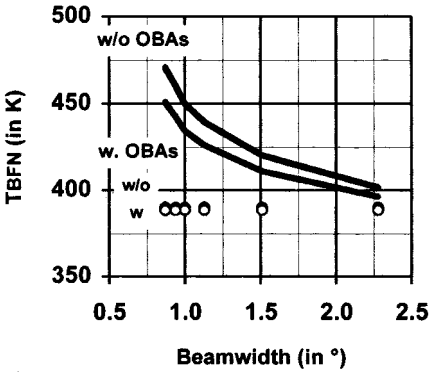

(b)

Fig. 7. Characteristic BFN parameters of the reconfigurable spotbeam antenna using active weighting BFNs with and without OBAs and equivalent passive-weighting versions. (a) BFN gain parameters. (b) BFN noise temperature. —— Active weighting BFNs. o o o passive weighting BFNs.

For the equivalent passive weighting BFN, the same nominal gains G_0 (18 dB without and 36 dB with OBAs), the same nominal noise temperatures T_e (381.4 K without and 388.5 K with OBAs), and the same ohmic path losses L_p of the combiner (4.5 dB per channel) are assumed leading to an overall combiner loss L_C of 13.0 dB [(33)] and an effective combiner temperature of 536.4 K [(34)].

The characteristic parameters G_{BFN} and T_{BFN} of the entire active weighting BFN, calculated according to (25a), (28), and (35), are shown in Fig. 7(a) and (b), together with the corresponding figures for the passive weighting equivalent, calculated according to (31a) and (32a). For an increase of the implemented beamwidth from 0.9° to 2.3° corresponding to a decrease of the ringtaper L_R from 17.3 dB to 2.7 dB, the normalized weighting gain G_W/N increases from -8.0 dB to -2.2 dB [Fig. 7(a)], which leads to an increase of the BFN gain for the active weighting case from 22.9 dB to 28.7 dB for the basic configuration and from 4.9 dB to 10.7 dB for the alternative version without OBAs. This illustrates that an increasing amplitude taper implies in fact a degradation of the active weighting BFN gain, as mentioned in Section III, whereby the BFN version without OBAs achieves always 18 dB less BFN gain because of the missing OBA amplification. The equivalent passive weighting BFNs achieve a constant BFN gain of 13.5 dB without and 31.5 dB with OBAs, i.e., they operate always with maximum BFN gain as discussed in Section III.

The corresponding BFN noise temperatures [Fig. 7(b)] decrease from 451.3 K to 396.5 K for the basic active weighting configuration and from 471.1 K to 401.8 K for the alternative, if the beamwidth is increased as described before. Since the OBAs reduce the impact of the combiner noise on T_{BFN}, slightly better figures are obtained for the basic configuration but, in general, both cases do neither exhibit excessive differences nor a very strong sensitivity to the applied amplitude setting. The equivalent passive weighting BFNs provide a constant BFN noise temperature of 389.9 K without and 388.6 K with OBAs, i.e., they

operate always with minimum BFN temperature as discussed in Section III.

The available overall antenna gain at the ARI [(15)] as well as the effective system noise temperature referred to the interface "0" and the overall G/T of the antenna/receiver combination [(16)] are shown in Fig. 8(a)–(c), respectively. Hereby, a total radiator system loss $L_A = 1.0$ dB covering the losses of the reflector, the horn/polarizer assemblies and the connecting waveguides at 30 GHz, and a receiver/input-waveguide assembly with an input noise temperature of $T_{\text{rec}} = 1200$ K ($N_F = 7.0$ dB) have been assumed.

For the overall antenna gain of the active weighting configuration, Fig. 8(a) shows an almost constant gain of 63.3–62.5 dB (with OBAs) and 45.3–44.5 dB (without OBAs), which is a consequence of the fact that a beamwidth increase from 0.9° to 2.3° (L_R decrease from 17.3 dB to 2.7 dB) leads to an increase of the BFN gain but an almost equal decrease of the directivity. Here, the two effects are able to compensate each other leading to an overall gain variation of only 0.8 dB for a beamwidth variation of about 1 : 2.6. This effect has been verified experimentally during a classified EHF antenna development and is a special property of single-reflector (or lens) multifeed antennas with active weighting BFNs, whereas directivity and BFN gain changes add-up for direct radiating or magnified arrays using such networks. The effect can be important for the specification of the receiver input dynamic range which has to cover both the dynamic range of the incoming signals, as well as any gain variation of the antenna. For the passive weighting equivalents, also shown in Fig. 8(a), the BFN gain is constant as discussed before, i.e., the variation of the overall gain follows the directivity change without any compensation leading to a gain decrease from 71.8 dB to 65.3 dB (with OBAs) and from 53.8 dB to 47.3 dB (without OBAs). Like the directivity, the variation of the overall gain is about 6.5 dB for beamwidth of 0.9° to 2.3°, which has to be taken into account for the specification of the receiver. As aforementioned, the passive-weighting configuration delivers higher gain values for comparable electronic gains due to the quasi-lossless implementation of the amplitude weighting, which can be compensated, however, by an increase of the chain gains for active weighting configurations.

The effective system noise temperatures T_{sys} of the antenna/receiver combination referred to the interface "0" are presented in Fig. 8(b) assuming a total received antenna noise of $T_A = 300$ K which typically occurs if a narrow-beam satellite antenna is pointed toward a warm, dry land mass. For the active weighting configuration with OBAs, T_{sys} is fairly constant with figures between 952.2 K and 877.6 K, whereas the corresponding version without these amplifiers shows a fairly significant increase from 1010.7 K to 1455.3 K for decreasing beamwidth. This effect is a consequence of a stronger receiver noise impact which is due to a low BFN gain for narrow beams (i.e., strong amplitude tapers) and missing OBAs. This impact is neither significant for the active-weighting configuration with OBAs nor for the passive-weighting BFNs, which obtain constant system noise temperatures of 934.7 K (without OBAs) and 866.7 K (with OBAs).

Finally, the G/T of the antenna/receiver combination is presented in Fig. 8(c) based again on the assumption of a total received antenna noise of $T_A = 300$ K. Since T_{sys} is similar for the active weighting case with OBAs and the two passive weighting configurations having a similar and fairly small variation with the beamwidth, the obtained G/T figures of 11.6 dB/K to 5.4 dB/K for the active weighting case, 11.6 dB/K to 5.1 dB/K for the passive-weighting case without OBAs, and 12.0 dB/K to 5.4 dB/K for the passive-weighting case with OBAs are also similar

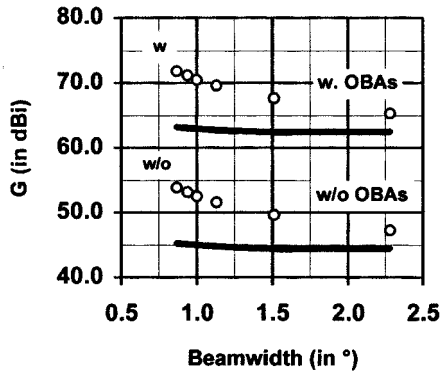

(a)

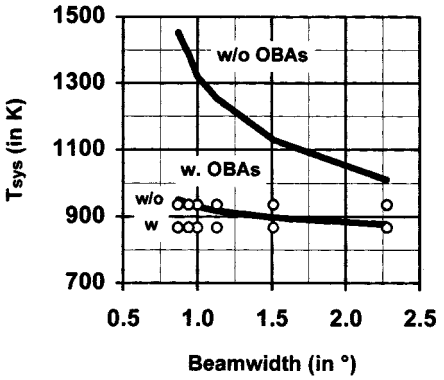

(b)

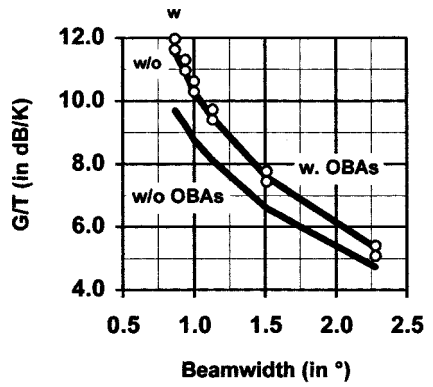

(c)

Fig. 8. Gain, system noise temperature, and G/T-performance of the reconfigurable spotbeam antenna using active weighting BFNs with and without OBAs and equivalent passive weighting versions. (a) Overall antena gain at the ARI. (b) System noise temperature at the interface "0" for the antenna connected to a receiver with $T_{\text{rec}} = 1200$ K. (c) G/T for the antenna connected to a receiver with $T_{\text{rec}} = 1200$ K. —— Active weighting BFNs. o o o passive weighting BFNs.

and show a dependence on the selected beamwidth, which is mainly driven by the directivity change of about 6.5 dB over the considered beamwidth range. In case of the active-weighting BFN without OBAs, G/T reaches only 9.7 dB/K to 4.7 dB/K because of the stronger increase of T_{sys}, shown in Fig. 8(b). Overall, the total G/T-improvement obtained via the use of OBAs is about 1.8 dB for the narrowest beam (strongest amplitude taper) and reduces to about 0.6 dB for widest beam in case of the active-weighting BFNs, whereas it remains about 0.3 dB for all beamwidths in case of the passive-weighting alternatives.

V. Summary and Conclusion

A basic system-level model for the gain and G/T of active multielement receive antennas has been presented that covers arbitrary beamforming networks and direct radiating arrays, as well as array-fed systems with one or more focussing elements (reflectors or lenses). In particular, the most common case of identical chains for each radiating element and a separability into a passive radiator system and an active BFN have been discussed in detail together with a brief overview of measurement possibilities for the characteristic model parameters. This basis of useful, measurable parameters, which are consistent with conventional communication system analysis methods, is seen as the main advantage of the presented model that permits its application to the analysis and design of systems using active multielement antennas and to the specification, design, and test of such antennas as well.

The characteristic BFN parameters G_{BFN} and T_{BFN} have been derived and discussed for a generic beamforming network and the two most popular configurations called active-weighting and passive-weighting architecture. For these architectures, general power combiners, as well as their most common implementations, have been considered. A comparison of active and passive weighting has shown, that the active weighting configuration offers more flexibility at the expense of a performance degradation in terms of gain and noise temperature for increased amplitude weightings. This degradation can be minimized, however, by a suitable BFN design providing sufficient electronic amplification. In contrast, the passive weighting architecture offers very limited or no reconfiguration possibilites for the provided amplitude distribution but operates always with maximum BFN gain and minimum BFN noise temperature.

The obtained general results have been illustrated by simulations for a multifeed Ka-band reflector antenna, where the beamwidth can be selected between 0.9° and 2.3° through the use of a suitable beamforming network. For reasons of comparison, both active-weighting BFNs offering full beamwidth flexibility, as well as passive-weighting equivalents for limited switchable beamsizes, have been considered. Whereas active-weighting BFNs cause a compensation of the directivity and BFN gain changes leading to a change of the overall antenna gain of only 0.8 dB over a beamwidth variation of about 1 : 2.6, passive-weighting BFNs deliver a higher absolute gain and cause a gain change according to the directivity variation of about 6.5 dB. The described compensation effect is of advantage for the dynamic range of the following receiver, but is limited to array-fed antennas with one focusing element, whereas directivity and BFN gain changes add-up for direct radiating or magnified arrays. In terms of system-noise temperature, both active- and passive-weighting BFNs deliver similar performances with a low sensitivity to the selected amplitude setting provided that the active weighting architecture uses a sufficiently high internal amplification. Consequently, the obtained G/T-figures are also similar having a dynamic driven by the directivity changes of about 6.5 dB, whereas active weighting BFNs with a poor internal amplification show an additional degradation which is most critical for the narrowest beams, i.e., the most significant amplitude tapers.

Finally, it should be noted that the validity of the presented model, as well as the predicted key effects, have been verified experimentally during a classified antenna development at EHF-frequencies. Due to the nature of such projects, however, the detailed results of these measurements cannot be reported here.

Appendix
Antenna Temperature T_A for Coherent and Noncoherent Cases

As discussed in Sections I and II, the impact of noise received by a multielement antenna is described by the conventional antenna noise temperature or radiometric antenna temperature T_A [1], which is given by

$$T_A = \iint_{4\pi} T_{AP}(\theta, \phi) F_n(\theta, \phi)\, d\Omega \Big/ \iint_{4\pi} F_n(\theta, \phi)\, d\Omega \quad \text{(A1)}$$

with T_{AP} and F_n being the apparent noise temperature distribution seen by the antenna and the antenna pattern, respectively [1]. Though this formulation basically applies to all types of antennas, the antenna pattern to be used in (A1) depends on the system bandwidth, if multielement (array) antennas are considered.

If the bandwidth of the considered system is comparably small, which applies to most communication systems, the noise received by the individual antenna elements can be treated like additional signals (coherent case), i.e., the same overall (array) antenna pattern applies to both signals and received noise and is used in (A1) in order to derive T_A. If a low sidelobe pattern is generated, for example, external noise sources located in sidelobe directions do not affect T_A because corresponding noise contributions received by individual elements are cancelled out within the BFN in the same way as corresponding signals coming from those directions.

If the bandwidth of the considered system is very large, which applies to some radar applications, the situation is more complex, since here the received noise must be treated in the same way as the internal noise sources of the antenna (noncoherent case). In this case, the noise received by *each antenna element* can be described by individual antenna temperatures $T_{A,1}$ to $T_{A,N}$ which are derived from (A1) using the individual *in situ* element pattern for F_n. Taking the antenna model shown in

Fig. 2 and replacing the parameter $T_{\rm in}$ by these individual noise temperatures, the output noise temperature $T_{\rm out}$ is given by

$$T_{\rm out} = (T_A + T_{\rm act})G_{\rm act} = \sum_{n=1}^{N} (T_{A,n} + T_n)G_n \qquad \text{(A2)}$$

[cf. (11)], which leads to

$$T_A = \sum_{n=1}^{N} T_{A,n}G_n \Big/ \sum_{n=1}^{N} G_n \qquad \text{(A3)}$$

using (10) and (12). If all elements see the same apparent noise temperature distribution T_{AP} and have sufficiently similar *in situ* radiation pattern F_n which applies to most applications, the individual antenna temperatures $T_{A,n}$ are equal leading to

$$T_{A,1} = T_{A,2} = \cdots = T_{A,N} = T_A \qquad \text{(A4)}$$

i.e., the antenna temperature of the multielement (array) antenna is given by the antenna temperature of the single antenna elements. In this case, a cancellation of noise contributions from different elements is not possible since noncorrelated noise simply adds-up in the BFN power combiner which implies that even for a low sidelobe (signal) pattern, noise sources located in sidelobe directions can significantly affect the overall antenna temperature T_A as long as the element pattern do not vanish for those directions. This effect can be a particular problem for low sidelobe direct radiating arrays where low-gain antenna elements are used having a wide field of view.

ACKNOWLEDGMENT

The author would like to aknowledge the support of D. U. E. Blaschke of Dornier Satellite Systems (DSS), Munich, Germany, who performed the directivity and pattern computations for the presented application example. Furthermore, the author thanks the DSS SATCOM development team and especially M. Weber, W. Lindemer, and H. Wolf for their contribution to the underlying classified experiments.

REFERENCES

[1] F. T. Ulaby, R. K. Moore, and A. K. Fung, *Microwave Remote Sensing*. Reading, MA: Addison-Wesley, 1981, vol. 1, sec. 4–5.3, pp. 203–205.
[2] A. J. Simmons and D. G. Bodnar, "Gain of active antenna systems: Antenna standards comittee requests inputs," *IEEE AP-S-Newslett.*, p. 62, Oct. 1989.
[3] G. E. Evans, *Antenna Measurement Techniques*. Norwood, MA: Artech House, 1990, pp. 68–73.
[4] J. J. Lee, "G/T and noise figure of active array antennas," *IEEE Trans. Antennas Propagat.*, vol. 41, pp. 241–244, 1993.
[5] E. L. Holzman and A. K. Agrawal, "A comparison of active phased array, corporate beamforming architectures," in *Proc. IEEE Int. Symp. Phased-Array Syst. Technol.*, Boston, MA, 1996, pp. 429–433.
[6] U. R. Kraft and D. U. E. Blaschke, "Gain and G/T-considerations on spaceborne active receive antennas," in *Proc. IEEE Int. Symp. Antennas Propagat.*, Montréal, Canada, 1997, pp. 2468–2471.
[7] U. R. Kraft, "Satellite antennas for future military communications at EHF," in *Proc. Symp. Concepts Post-NATO IV Satcom Syst.*, vol. II, den Haag, The Netherlands, 1995, Paper SP-11.
[8] U. R. Kraft, H. Wolf, and E. Sommer, "Steerable antennas and arrays for satellite communications (in German: Steuerbare Antennen und Gruppenantennen für die Satellitenkommunikation)," in *Proc. 1 DARA Workshop Satellite Commun.*, Bad Neuenahr, Germany, 1996, pp. 209–215.
[9] W. Bornemann, M. Trümper, and L. Jensen, "INTELSAT VIII Antennas," in *Proc. JINA 94*, Nice, France, 1994, pp. 167–173.
[10] L. Jensen, W. Chang, E. Dudok, C. Hunscher, B. Sauerer, N. Schröder, E. Sommer, and H. Wolf, "The INTELSAT 8 Antenna Subsystem," in *Proc. ITG Conf. Antennas*, Munich, Germany, 1998, pp. 47–52.

Ulrich R. Kraft (M'89–SM'97) received the Dipl.-Ing. and Dr.-Ing. degrees in electrical engineering (both *summa cum laude*) from the Technical University Berlin (TUB), Germany, in 1986 and 1988, respectively.

From 1985 to 1989, he was a Research Associate at the Microwave Institute of the TUB where he conducted research on fundamental aspects of the description and optimization of circularly polarized antennas such as helix antennas, spiral antennas, microstrip patch antennas and sequetially rotated arrays. Since 1989, he is with MBB/Space Division, Munich and its successors such as DaimlerChrysler Aerospace and now Astrium GmbH, where he served in various engineering, marketing/strategy and management positions. He has published about 35 scientific papers and conference contributions. His professional fields of activities cover technology developments for spaceborne atmospheric sensors operating in the THz regime, the theory of passive aperture synthesis radiometry and its application to spaceborne surface sensors, as well as the theory and application of reconfigurable active array antennas for satellite communication.

Dr. Kraft received the Karl-Ramsauer Research Award in 1989. He currently serves as referee for professional journals such as *Electromagnetics* and the *IEE Proceedings* as a member of the IEEE MTT/AP German Chapter Commission and as the editor of the MTT/AP German Newsletter.